

Received November 18, 2018, accepted November 24, 2018, date of publication November 27, 2018,
date of current version December 27, 2018.

Digital Object Identifier 10.1109/ACCESS.2018.2883689

Non-Rigid Point Set Registration via Adaptive Weighted Objective Function

CHANGCAI YANG^{ID}^{1,2}, YIZHANG LIU^{1,2}, XINGYU JIANG³, ZEJUN ZHANG^{1,2},
LIFANG WEI^{1,2}, TAOTAO LAI^{ID}^{1,2}, AND RIQING CHEN^{1,2}

¹Digital Fujian Research Institute of Big Data for Agriculture and Forestry, College of Computer and Information Science, Fujian Agriculture and Forestry University, Fuzhou 350002, China

²Key Laboratory of Smart Agriculture and Forestry, Fujian Province University, Fujian Agriculture and Forestry University, Fuzhou 350002, China

³Electronic Information School, Wuhan University, Wuhan 430072, China

Corresponding author: Xingyu Jiang (e-mail: jiangx.y@whu.edu.cn)

This work was supported in part by the National Natural Science Foundation of China under Grant 61501120, Grant 61701117, and Grant 61702101, in part by the Outstanding Youth Research Talent Cultivation Program Colleges and Universities in Fujian Province and in Fujian Agriculture and Forestry University under Grant XJQ201514, and in part by the Natural Science Fund of Fujian Province under Grant 2017J01736.

ABSTRACT Non-rigid point set registration is a fundamental problem in many fields related to computer vision, medical image processing, and pattern recognition. In this paper, we develop a new point set registration method by using an adaptive weighted objective function, which formulates the alignment of two point sets as a mixture model estimation problem. The correspondences and the transformation are jointly recovered by using the expectation–maximization algorithm to obtain the promising results. First, the correspondences are established using local feature descriptors, and the adaptation parameters for the mixture model are computed from these correspondences. Then, the underlying transformation is recovered by minimizing the adaptive weighted objective function deduced from the mixture model. We demonstrate the advantages of the proposed method on various types of synthetic and real data and compare the results against those obtained using the state-of-the-art methods. The experimental results show that the proposed method is robust and outperforms the other registration approaches.

INDEX TERMS Registration, expectation-maximization (EM) algorithm, thin-plate spline (TPS), objective function, mixture model, point set.

I. INTRODUCTION

Registration of point sets is an important fundamental and challenging research area widely employed in many fields related to computer vision [1]–[7]. With a salient structure represented by the points, many applications in these fields, such as image fusion [8], structure computation [9], and image point correspondence [10], can be typically considered as point set registration problems [3]. The point set registration aims to find the correct point matches between two sets of key-points extracted from the input data and to identify the underlying transformation that warps one point set to the other.

To align the two point sets accurately, many methods have been proposed in the past few decades. Depending on the applications and the different characteristics of the data, two main approaches, namely rigid or non-rigid registration, to point set registration have been developed. Rigid point set registration is relatively easy as it contains only

rotation, scaling, and translation. Numerous point set registration approaches, (e.g., [3], [4], [11]) have been proposed. Most of them can achieve excellent performance. In contrast, handling the non-rigid registration issue is very complex in that the underlying non-rigid spatial transformation, which allows scaling and anisotropic skews, is usually complicated, unknown, and difficult to model [5]. However, non-rigid registration is a problem of critical importance in computer vision as it has been faced in a considerable variety of real-world tasks, such as shape classification [12], [13], medical image mosaic [1], [13], visual navigation [14], and hand-written character recognition [15], and so on.

To illustrate the problem addressed in this paper, an example of a simple alignment of two point sets is shown in Fig. 1. As shown in Fig. 1(b), we cope with the data (i.e., the correspondences between two sets of points). A non-rigid point set registration method aims to estimate the underlying transformation that aligns the model point set onto the target point

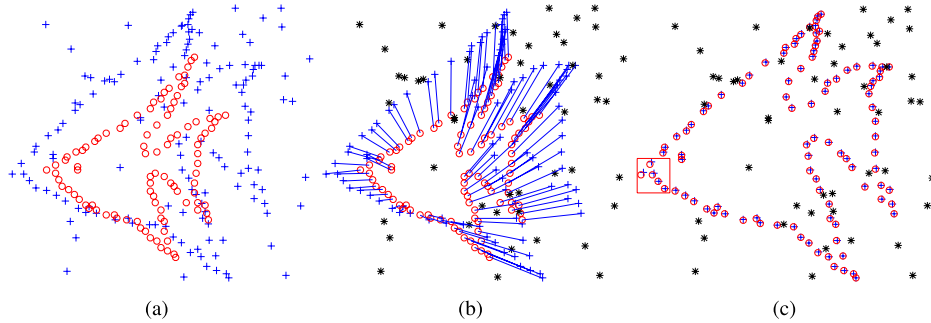


FIGURE 1. An example of the non-rigid point set registration. (a) Point sets of the model (red circles) and target (blue pluses) shapes. (b) Correspondences between two sets of points and outliers (black star). (c) Registration result.

set and identifies the inliers (i.e., the points marked using red circles and blue plus signs in Fig. 1(c)) and the outliers (i.e., the points marked with black stars in Fig. 1(c)).

Many methods have been presented to handle the above mentioned problem. The Iterated Closest Point (ICP) is a popular point registration approach for matching the two point sets due to its simplicity and effectiveness. The ICP uses an iterated optimization method to solve the correspondence and the underlying transformation. In this iterative process, a binary correspondence recovered by using the nearest-neighbor relationships is used to refine the estimated transformation, and vice versa. The main limitation of this algorithm is that the binary correspondence generates a number of local minima. The performance of ICP will degenerate quickly when input data contain outliers. To overcome the drawback of ICP due to the binary response, a soft-assignment algorithm for the optimal correspondences between the two point sets was proposed by Chui and Rangarajan [5]. They present a general framework to match non-rigid points. The soft assignment and the non-rigid transformation are jointly solved by using the deterministic annealing technique. This approach is considerably similar to the expectation-maximization (EM) algorithm and outperforms ICP. Belongie *et al.* [15] developed a rich descriptor called shape context (SC) for shape matching. The SC, which captures the distribution of the relative positions between the reference point and the remaining points, is used for solving the correspondence problem. The aligning transform is recovered using the correspondence. However, this approach ignores robustness when it estimates the spatial mapping from the correspondence.

To address the robustness issue, various methods have been proposed. Myronenko and Song [16] proposed a coherence point drift (CPD) algorithm for both rigid and no-rigid point set registration. They formulate the point matching problem as a probability density estimation problem and more specifically, a Gaussian mixture model (GMM) is used to represent one point set to the other one. GMM is robust even when input data contain missing points, noise, and outliers. In order to capture spatially asymmetric distributions, Dou *et al.* [17] use the asymmetric Gaussian model to represent the point sets. Zhou *et al.* [18] proposed a point registration method based

on Student's-t mixture model. They formulate the various mixture proportion as Dirichlet distribution and assign them to corresponding mixture components. A vector field consensus algorithm for point matching was proposed by Ma *et al.* [19], [20]. They explore the idea of considering the point correspondence as a vector field interpolation between the two point sets. Zhou *et al.* [21] proposed a probabilistic inference method based on global and local regularizations for nonrigid feature matching. Yan *et al.* [22] proposed multi-graph matching algorithms based on the composition based optimization procedure. Recently, Lian *et al.* [23] proposed a globally optimal algorithm for point matching. They formulate the matching problem as a concave quadratic assignment problem with a few nonlinear terms by eliminating the transformation variables. A normal rectangular branch-and-bound approach based on rectangular subdivision is used to compute the optimal solution. More recently, an adaptive discrete hypergraph matching was proposed by Yan *et al.* [24]. They iteratively update the higher-order assignment by a linear assignment approximation. Yang *et al.* [13] introduced robust point registration approaches based on the local geometrical preserving. To preserve the local structure of point set, Bai *et al.* [25] formulate the local constraint with k-connected neighborhood as weighted least square error item. Other related work includes GMM based method [26], locally linear transforming based method [27], [28], and guided locality preserving feature matching method [7].

Carefully observing the red rectangular region in Fig. 1(c), we can find that some registration results are perfect and the others are not. The problem is the following: May equal using all these correspondences to recover the underlying transformation always produce optimal results? Obviously, the answer is no. Therefore, it is reasonable to assume that if the contribution of each correspondence to the final transformation is adaptively determined in the registration error, the registration results may be further accurate. In this paper, we present an adaptive weighted objective function for the alignment of two point sets, in which the non-rigid point set registration is formulated as a mixture model estimation problem. We recover both the correspondences and the underlying mapping by using the expectation-maximization (EM) algorithm. Firstly, a local feature such as

SC is used to establish the correspondences between the two point sets. The mixture weights for GMM are obtained from these correspondences. Then, the underlying transformation is computed by minimizing an adaptive weighted objective function developed from the mixture model. Moreover, the thin-plate spline (TPS) [29] is used to model the spatial mapping between the two point sets.

The rest of the paper is constructed as follows: Section 2 presents the proposed adaptive weighted objective function for the non-rigid registration, which can robustly recover the transformations from the contaminated correspondences. The point registration results are provided in Section 3, and the conclusions are drawn in Section 4.

II. METHOD

In this section, we consider the non-rigid point set registration problem as the estimation of the mixture-density parameters and recover the underlying transformation by minimizing the adaptive weighted objective function deduced from the mixture model. We also present the implementation details.

A. MIXTURE MODEL

Given two point sets - the model point set $\mathbf{X} = \{\mathbf{x}_j, j = 1, \dots, M\}$ with point $\mathbf{x}_j = (\mathbf{x}_j^x, \mathbf{x}_j^y, 1)$ and the target point set $\mathbf{Y} = \{\mathbf{y}_i, i = 1, \dots, N\}$ with point $\mathbf{y}_i = (\mathbf{y}_i^x, \mathbf{y}_i^y, 1)$ - our goal is to align \mathbf{X} to \mathbf{Y} by computing a coherent transformation \mathbf{T} that warps the model points to the target points. In this paper, we formulate the alignment of the two point sets as the mixture-density parameter estimation, where \mathbf{Y} represents the observed data points from a Gaussian distribution and the transformed $T(\mathbf{X})$ represents the GMM centroids.

Because of input data containing the missing points, the noise, and the outliers, it is desirable to have a robust estimation of \mathbf{T} . To this end, we assume that, the inlier distribution is a multivariate Gaussian distribution with equal isotropic covariances $\sigma^2 \mathbf{I}$; the outlier distribution is uniform with a constant $\frac{1}{a}$. Thus, the mixture model for the observed data points is as follows:

$$\begin{aligned} P(\mathbf{Y}|\mathbf{X}, \boldsymbol{\theta}) &= \prod_{i=1}^N P(\mathbf{y}_i|\boldsymbol{\theta}) \\ &= \prod_{i=1}^N \left[\gamma \sum_{j=1}^M \frac{\tau_{ij}}{(2\pi\sigma^2)^{D/2}} e^{-\frac{\|\mathbf{y}_i - \mathbf{T}(\mathbf{x}_j)\|^2}{2\sigma^2}} + (1-\gamma) \frac{1}{a} \right], \quad (1) \end{aligned}$$

where $\boldsymbol{\theta} = \{\mathbf{T}, \sigma^2, \gamma\}$ includes a set of unknown parameters and γ is the mixing coefficient that specifies the marginal distribution over the latent variable, i.e., $\forall z_i, P(z_i = j) = 1 - \gamma, 1 \leq j \leq M$. $z_i \in \{0, 1\}$ is a latent variable of the i -th sample, where $z_i = j, 1 \leq j \leq M$ indicates a Gaussian component and $z_i = M + 1$ points to a uniform distribution. τ_{ij} with $\sum_{j=1}^M \tau_{ij} = 1$ is the membership probability of the GMM. The matrix $\{\tau_{ij}\}$ is the correspondence matrix consisting of two parts. If a point \mathbf{x}_j corresponds to a point \mathbf{y}_i , $\tau_{ij} = \rho$;

otherwise $\tau_{ij} = (1 - \rho)/M$, where $0 \leq \rho \leq 1$. If a point \mathbf{x}_j does not have a corresponding model point, $\tau_{ij} = \frac{1}{M}$.

In general, the true parameter set $\boldsymbol{\theta}$ can be obtained by maximizing the likelihood function (1). The maximum likelihood estimation of $\boldsymbol{\theta}$, i.e., $\boldsymbol{\theta}^* = \arg \max_{\boldsymbol{\theta}} P(\mathbf{Y}|\mathbf{X}, \boldsymbol{\theta})$, can be determined by minimizing the negative log posterior

$$E(\boldsymbol{\theta}) = -P(\mathbf{Y}|\mathbf{X}, \boldsymbol{\theta}) = -\sum_{n=1}^i \ln P(\mathbf{y}_i|\boldsymbol{\theta}). \quad (2)$$

The coherent transformation \mathbf{T} can be directly achieved from the optimal solution $\boldsymbol{\theta}^*$.

B. ADAPTIVE WEIGHTED OBJECTIVE FUNCTION

Similar to the standard notations [30], some terms independent of $\boldsymbol{\theta}$ are omitted. Then, the complete-data log-likelihood function (2) becomes

$$\begin{aligned} Q(\boldsymbol{\theta}, \boldsymbol{\theta}^{old}) &= \frac{1}{2\sigma^2} \sum_{i=1}^N \sum_{j=1}^M p_{ij} \|\mathbf{y}_i - \mathbf{T}(\mathbf{x}_j)\|^2 \\ &\quad + \frac{\mathbf{NpD}}{2} \ln(\sigma^2) - \mathbf{Np} \ln(\gamma) \\ &\quad - (\mathbf{N} - \mathbf{Np}) \ln(1 - \gamma). \end{aligned} \quad (3)$$

where $p_{ij} = P(z_i = j|\mathbf{y}_i, \boldsymbol{\theta}^{old})$ is a soft decision, which indicates the degree to which the observed data point \mathbf{y}_i coincides with the model point \mathbf{x}_j under the current estimated transformation \mathbf{T} , and $\mathbf{Np} = \sum_{i=1}^N \sum_{j=1}^M p_{ij}$. Here, two unknown variables have to be solved: parameter set $\boldsymbol{\theta}$ and the responsibility p_{ij} . As $\boldsymbol{\theta}$ estimation requires p_{ij} and vice versa, it is natural to consider an alternative method. In this paper, we used the well-known EM algorithm [31] to solve this problem. It iterates, alternately, with an expectation step (E-step), which estimates p_{ij} under the given $\boldsymbol{\theta}$, and a maximization step (M-step), which updates $\boldsymbol{\theta}$ on the basis of the current estimate of p_{ij} . This new $\boldsymbol{\theta}$ is used to determine p_{ij} in the next E-step.

E-step: Denote \mathbf{P} as a posterior probability matrix of size $N \times M$. p_{ij} is determined by the Bayes rule, i.e.,

$$\begin{aligned} p_{ij} &= \frac{P(\mathbf{y}_i|z_i = j, \boldsymbol{\theta}^{old})P(z_i = j|\boldsymbol{\theta}^{old})}{P(\mathbf{y}_i|\boldsymbol{\theta}^{old})} \\ &= \frac{\tau_{ij} e^{-\frac{\|\mathbf{y}_i - \mathbf{T}(\mathbf{x}_j)\|^2}{2\sigma^2}}}{\sum_{k=1}^M \tau_{ik} e^{-\frac{\|\mathbf{y}_i - \mathbf{T}(\mathbf{x}_k)\|^2}{2\sigma^2}} + \frac{(2\pi\sigma^2)^{D/2}(1-\gamma)}{a\gamma}}. \end{aligned} \quad (4)$$

M-step: Reestimate the parameter set $\boldsymbol{\theta}^{new}$ as follows: $\boldsymbol{\theta}^{new} = \arg \max_{\boldsymbol{\theta}} Q(\boldsymbol{\theta}, \boldsymbol{\theta}^{old})$. Taking the derivative of $Q(\boldsymbol{\theta})$ with respect to γ and setting to zero gives

$$\gamma = \mathbf{Np}/N, \quad (5)$$

Similar to γ , σ^2 can be obtained as follows:

$$\sigma^2 = \frac{\sum_{i=1}^N \sum_{j=1}^M p_{ij} \|\mathbf{y}_i - \mathbf{T}(\mathbf{x}_j)\|^2}{\mathbf{NpD}}, \quad (6)$$

Next, we consider the term $\mathcal{Q}(\theta)$ with respect to \mathbf{T} . We obtain a weighted empirical error as follows:

$$\mathcal{E}(\mathbf{T}) = \frac{1}{2\sigma^2} \sum_{i=1}^N \sum_{j=1}^M p_{ij} \| \mathbf{y}_i - \mathbf{T}(\mathbf{x}_j) \|^2. \quad (7)$$

TPS is commonly used for representing flexible coordinate transformations. It is the only spline that can be cleanly decomposed into a globally affine and a locally non-affine subspaces controlled by the coefficients \mathbf{A} and \mathbf{W} respectively [29]. Therefore, we model the transformation \mathbf{T} as TPS. TPS can be given by

$$\mathbf{T}(\mathbf{x}) = \mathbf{x} \cdot \mathbf{A} + \tilde{K}(\mathbf{x}) \cdot \mathbf{W}, \quad (8)$$

where the kernel function $\tilde{K}(\mathbf{r})$ is defined by the TPS kernel $\tilde{K}(r) = r^2 \log r$, and $\tilde{K}_{ij} = \tilde{K}(|\mathbf{x}_i - \mathbf{x}_j|)$. It is a powerful tool for recovering the transformation between shapes [5], [12], [15], [32].

However, solving the problem of (7) directly would yield an unstable solution, as there is noise in the specified values \mathbf{y}_i [15]. To overcome this problem, we impose the standard TPS regularization $\phi(\mathbf{W}) = \text{tr}(\mathbf{W}^T \mathbf{K} \mathbf{W})$ on T to control the complexity of the hypothesis space. This let us express the mapping \mathbf{T} estimation as the following minimizing problem

$$\Psi(\mathbf{T}) = \frac{1}{2\sigma^2} \sum_{i=1}^N \sum_{j=1}^M p_{ij} \| \mathbf{y}_i - \mathbf{T}(\mathbf{x}_j) \|^2 + \frac{\lambda}{2} \text{tr}(\mathbf{W}^T \mathbf{K} \mathbf{W}). \quad (9)$$

where the positive real number λ controls the amount of smoothing. The first term can be seen as an adaptive weighted objective function, where the weight p_{ij} is a data-dependent adaptation parameter under the given θ . The second smoothness term is independent on the affine components and is the bending energy.

Next, we substitute (8) into the expression (9), and then, obtain the following error function

$$\begin{aligned} \Psi(\mathbf{A}, \mathbf{W}) &= \frac{1}{2\sigma^2} \sum_{i=1}^N \sum_{j=1}^M p_{ij} \| \mathbf{y}_i - \mathbf{x}_j \mathbf{A} - \tilde{K}(\mathbf{x}_j) \mathbf{W} \|^2 \\ &\quad + \frac{\lambda}{2} \text{tr}(\mathbf{W}^T \mathbf{K} \mathbf{W}). \end{aligned} \quad (10)$$

The spatial mapping consensus problem is further rewritten as follows:

$$\begin{aligned} \mathcal{E}(\mathbf{A}, \mathbf{W}) &= \frac{1}{2\sigma^2} \sum_{i=1}^N \| (\mathbf{Y}_i^M - \mathbf{X}\mathbf{A} - \mathbf{K}\mathbf{W}) d(\mathbf{P}_i)^{1/2} \|^2 \\ &\quad + \frac{\lambda}{2} \text{tr}(\mathbf{W}^T \mathbf{K} \mathbf{W}) \\ &= \frac{1}{2\sigma^2} \| \mathbf{Y}\mathbf{P}^{1/2} - (\mathbf{X}\mathbf{A} - \mathbf{K}\mathbf{W}) d(\mathbf{P})^{1/2} \|^2 \\ &\quad + \frac{\lambda}{2} \text{tr}(\mathbf{W}^T \mathbf{K} \mathbf{W}) \\ &= \frac{1}{2\sigma^2} \| \tilde{\mathbf{Y}} - \tilde{\mathbf{X}} - \mathbf{K}\mathbf{W} d(\mathbf{P})^{1/2} \|^2 \\ &\quad + \frac{\lambda}{2} \text{tr}(\mathbf{W}^T \mathbf{K} \mathbf{W}). \end{aligned} \quad (11)$$

where $\tilde{\mathbf{X}} = \mathbf{X} d(\mathbf{P})^{1/2}$, $\tilde{\mathbf{Y}} = \mathbf{Y} \mathbf{P}^{1/2}$.

Following [5] and [29], a QR decomposition is used to clearly separate the warping into affine and non-affine subspaces. The QR decomposition of $\tilde{\mathbf{X}}$ is as follows:

$$\tilde{\mathbf{X}} = [\mathbf{Q}_1 \quad \mathbf{Q}_2] \begin{bmatrix} \mathbf{R} \\ \mathbf{0} \end{bmatrix}, \quad (12)$$

where \mathbf{Q}_1 is the orthonormal matrix of size $N \times 3$, \mathbf{Q}_2 is the orthonormal matrix of size $N \times (N - 3)$, and \mathbf{R} is the upper triangular matrix of size 3×3 . Then, equation (11) becomes

$$\begin{aligned} \mathcal{E}(\mathbf{A}, \Gamma) &= \frac{1}{2\sigma^2} (\| \mathbf{Q}_2^T \tilde{\mathbf{Y}} - \mathbf{Q}_2^T \mathbf{K} d(\mathbf{P})^{1/2} \mathbf{Q}_2 \Gamma \|^2 \\ &\quad + \| \mathbf{Q}_1^T \tilde{\mathbf{Y}} - \mathbf{R}\mathbf{A} - \mathbf{Q}_1^T \mathbf{K} d(\mathbf{P})^{1/2} \mathbf{Q}_2 \Gamma \|^2) \\ &\quad + \frac{\lambda}{2} \text{tr}(\Gamma^T \mathbf{Q}_2^T \mathbf{K} \mathbf{Q}_2 \Gamma), \end{aligned} \quad (13)$$

where $\mathbf{W} = \mathbf{Q}_2 \Gamma$ and Γ is a matrix of size $(N - 3) \times 3$. Taking the derivatives of $\mathcal{E}(\mathbf{A}, \Gamma)$ with respect to Γ and equating to zero yields the following

$$\frac{1}{2\sigma^2} (\mathbf{S}^T \mathbf{S} \Gamma - \mathbf{S}^T \mathbf{Q}_2^T \tilde{\mathbf{Y}}) + \frac{\lambda}{2} \mathbf{U} \Gamma = 0, \quad (14)$$

where $\mathbf{S} = \mathbf{Q}_2^T \mathbf{K} d(\mathbf{P})^{1/2} \mathbf{Q}_2$, $\mathbf{U} = \mathbf{Q}_2^T \mathbf{K} \mathbf{Q}_2$. From (14), we obtain the following:

$$\Gamma = \mathbf{Q}_2 (\mathbf{S}^T \mathbf{S} + \lambda \sigma^2 \mathbf{U} + \tilde{\epsilon} \mathbf{I})^{-1} \mathbf{S}^T \mathbf{Q}_2^T \quad (15)$$

where $\tilde{\epsilon} \mathbf{I}$ is used for numerical stability. Then \mathbf{W} is obtained as follows:

$$\mathbf{W} = \mathbf{Q}_2 \Gamma = \mathbf{Q}_2 (\mathbf{S}^T \mathbf{S} + \lambda \sigma^2 \mathbf{U} + \tilde{\epsilon} \mathbf{I})^{-1} \mathbf{S}^T \mathbf{Q}_2^T \tilde{\mathbf{Y}}, \quad (16)$$

The derivative with respect to \mathbf{A} yields the following

$$\mathbf{Q}_1^T \tilde{\mathbf{Y}} - \mathbf{R}\mathbf{A} - \mathbf{Q}_1^T \mathbf{K} d(\mathbf{P})^{1/2} \mathbf{W} = 0 \quad (17)$$

Then, \mathbf{A} is obtained as follows:

$$\mathbf{A} = \mathbf{R}^{-1} \mathbf{Q}_1^T (\tilde{\mathbf{Y}} - \mathbf{K} d(\mathbf{P})^{1/2} \mathbf{W}). \quad (18)$$

Thus, we obtain the underlying transformation \mathbf{T} in equation (8).

C. IMPLEMENTATION DETAILS

Invoking the non-rigid point set registration problem, we aim to estimate a non-rigid transformation \mathbf{T} that yields the best alignment between the model point set $\{\mathbf{x}_j\}_{j=1}^M$ and the target point set $\{\mathbf{y}_i\}_{i=1}^N$. The proposed approach solve both the matches and the transformation between the two point sets. For the point correspondences, the SC [15] is used as the feature descriptors. Then the χ^2 test statistic is used as the cost measure, and the Hungarian method is used to establish the putative correspondences between $\{\mathbf{x}_j\}_{j=1}^M$ and $\{\mathbf{y}_i\}_{i=1}^N$. The performance of the transformation estimation relies, typically, on the coordinate system in which the points are expressed. In this paper, data normalization is used to control this factor. For the point sets $\{\mathbf{x}_j\}$ and $\{\mathbf{y}_i\}$, we find two similarity transformations T_x and T_y , i.e. $\hat{\mathbf{y}}_j = T_y \mathbf{y}_j$, which ensure that the centroid of the points is at the coordinate

Algorithm 1 Non-Rigid Point Set Registration

Input: Two point sets $\{\mathbf{x}_j\}_{j=1}^M, \{\mathbf{y}_i\}_{i=1}^N$, and parameters λ, a
Output: Aligned model point set $\{T(\mathbf{x}_j)\}_{j=1}^M$

- 1 Normalization: $\hat{\mathbf{x}}_j = T_{\mathbf{x}} \mathbf{x}_j, \hat{\mathbf{y}}_i = T_{\mathbf{y}} \mathbf{y}_i$;
- 2 Compute feature descriptors for the target point set $\{\hat{\mathbf{y}}_i\}_{i=1}^N$;
- 3 Construct kernel matrix \mathbf{K} using the definition of K ;
- 4 Initialization: $\gamma = 0.5, \mathbf{W} = \mathbf{0}, \mathbf{A} = \mathbf{I}_{3 \times 3}, \sigma^2 = \frac{1}{NPD} \sum_{i=1}^N \sum_{j=1}^M \| \hat{\mathbf{y}}_i - T(\hat{\mathbf{x}}_j) \|^2$;
- 5 **repeat**
- 6 **E-step:**
- 7 Compute feature descriptors for the transformed $\{T(\hat{\mathbf{x}}_j)\}_{j=1}^M$;
- 8 Estimate the correspondence between $\{T(\hat{\mathbf{x}}_j)\}_{j=1}^M$ and $\{\mathbf{y}_i\}_{i=1}^N$ using the feature descriptors of the two point sets;
- 9 Update the responsibility p_{ij} using (4);
- 10 **M-step:**
- 11 Update \mathbf{W} and \mathbf{A} using equations (16) and (18);
- 12 Update transformed $\{T(\hat{\mathbf{x}}_j)\}_{j=1}^M$ using equation (8);
- 13 Update γ and σ^2 using equations (5) and (6);
- 14 **until** reach the maximum iteration number;
- 15 The aligned model point set $\{T(\mathbf{x}_j)\}_{j=1}^M$ is given by $T_{\mathbf{y}}^{-1} \{T(\hat{\mathbf{x}}_j)\}_{j=1}^M$ in the last iteration.

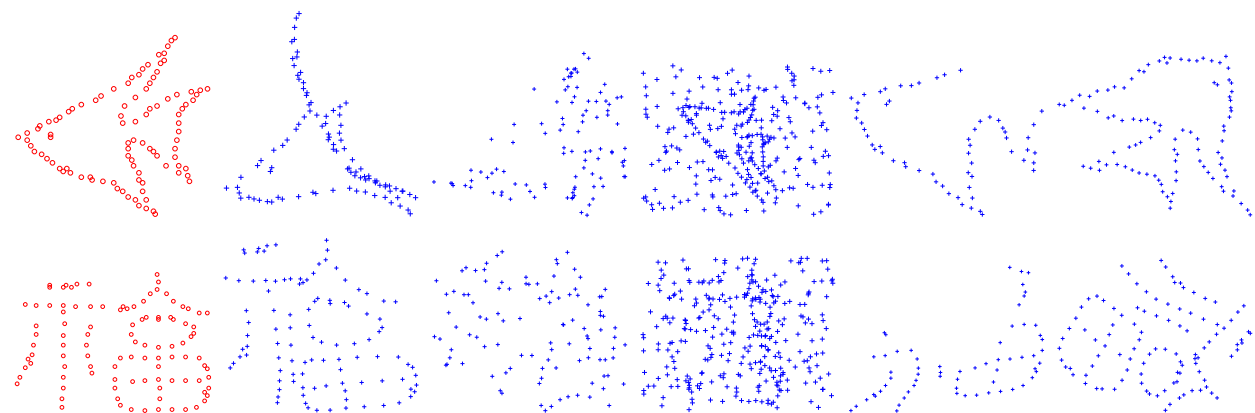


FIGURE 2. Sample synthetic data for evaluating the proposed point set registration method. The template point sets are shown in the left column. Examples of the target point sets in the deformation, noise, outlier, occlusion, and rotation tests are shown in columns 2-4, respectively. The shapes of the fish and the Chinese character are shown in the top row and the bottom row, respectively.

origin and the average distance from the origin is equal to $\sqrt{2}$ [9].

The regularization parameters λ and the uniform distribution parameter a are set to be 10 and 5, respectively. The proposed method is outlined in Algorithm 1.

The most relevant non-rigid point sets registration algorithm to ours is preserving global and local structures (PR-GLS), as both methods use the GMM formulation and the EM algorithm to recover both the correspondences and the underlying mapping. In PR-GLS algorithm, the reproducing kernel Hilbert space is used to model the spatial mapping. However, our method uses the TPS to parameterize the non-rigid spatial mapping. With the bending energy minimization, it can be decomposed into affine and non-affine subspaces. This may make for the non-rigid point sets registration. Moreover, the standard TPS regularization is used to control the complexity of the hypothesis space in our method.

III. EXPERIMENTAL RESULTS

To verify the proposed point set registration approach, we test it on various types of synthetic and real data and compare it to other state-of-the-art methods.

A. EXPERIMENTS WITH SYNTHESIZED DATA

To evaluate our proposed method, we first test it on the synthesized data set [5], which contains two kinds of shape models: the fish and the Chinese data sets. The fish and the Chinese data sets contain 96 and 108 points, respectively. For each shape model, five sets of data with different degenerations including deformation, noise, outlier, occlusion, and rotation are designed to test the performance of various registration algorithms. To analyze the influence of point set distortion, each above distortion is employed to a shape model to generate a target set, and 100 samples are created for each degradation level. Some examples from the synthetic data used in the experiments are shown in Fig. 2.

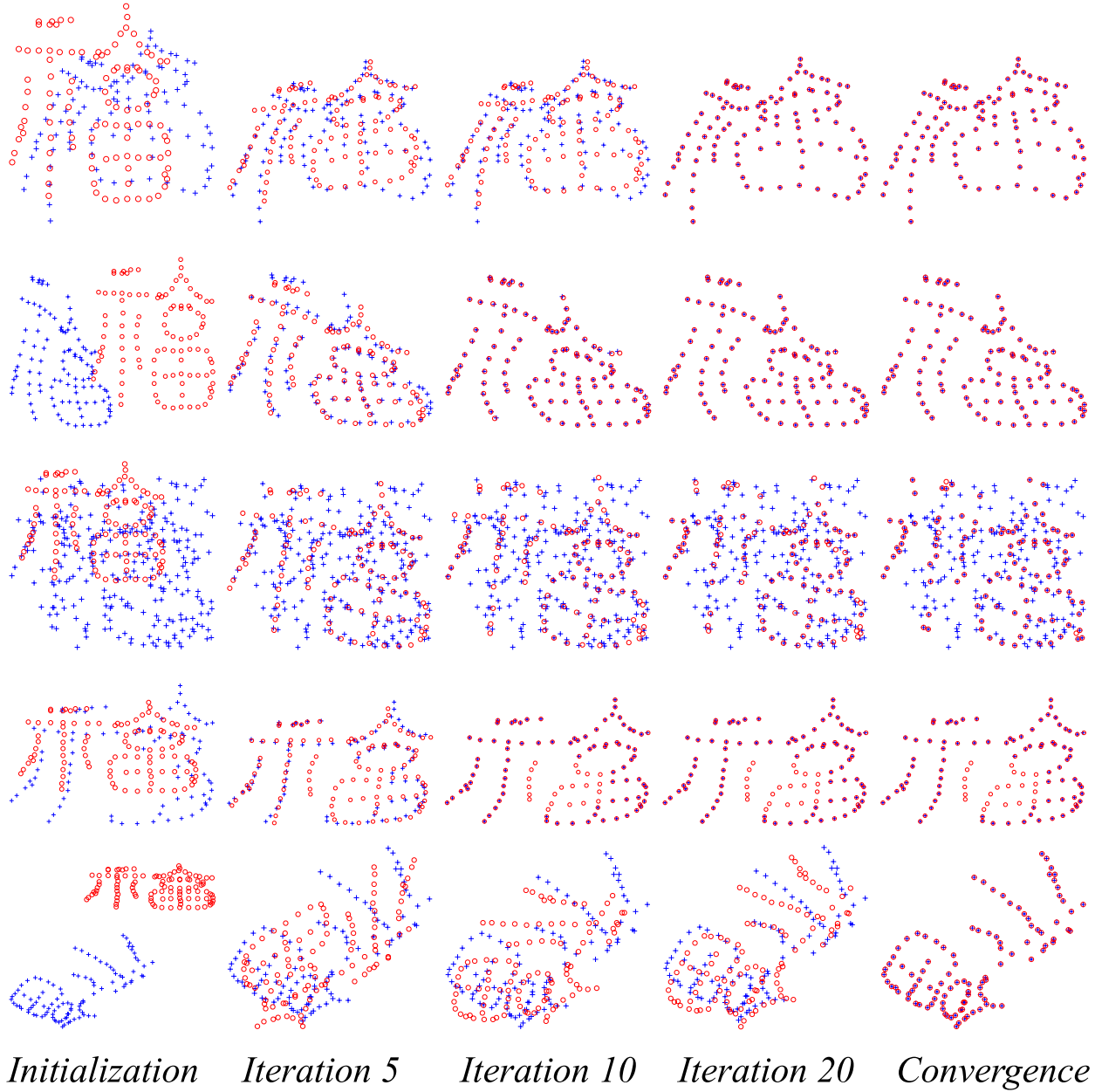


FIGURE 3. Illustration of registration progress of our method on Chinese character point sets. The aim is to align red circles onto blue pluses. Results on deformation, noise, outlier, occlusion, and rotation tests are shown in the top-down order, respectively. Results on various number of iterations are shown the left-right order.

Given two points, we first establish initial correspondences using SC [15]. For the rotation test, the rotation-invariant SC is used as in [33] when necessary. Fig. 3 illustrates the registration process of our approach on Chinese character point sets. Each row provides a different type of distortion, and the columns show the iterative alignment progress. We align the model point set (red circles) onto the target point set (blue plus signs). From Fig. 3, we can observe that the proposed method achieves good registration results, and it usually converges in 30 iterations.

We compare the performance of our method with that of seven state-of-the-art methods: SC [15], TPS-RPM [5],

CPD [16], COA-RPM [34], EM-TPS [12], MR-RPM [35], [36], and LPM [37]. The source codes of these competing methods are provided by their authors. The mean and standard deviation of the registration error of all the 100 samples are given in Figs. 4 and 5. The registration error on a pair of shapes is quantified as the average Euclidean distance between a point in the target and the corresponding point in the warped model. Some registration results obtained by the eight competing registration methods are also shown in Figs. 6 and 7. As shown in Figs. 4, 5, 6, and 7, the proposed method is robust and achieves accurate results on the synthesized data set, i.e., it achieves the lowest mean of

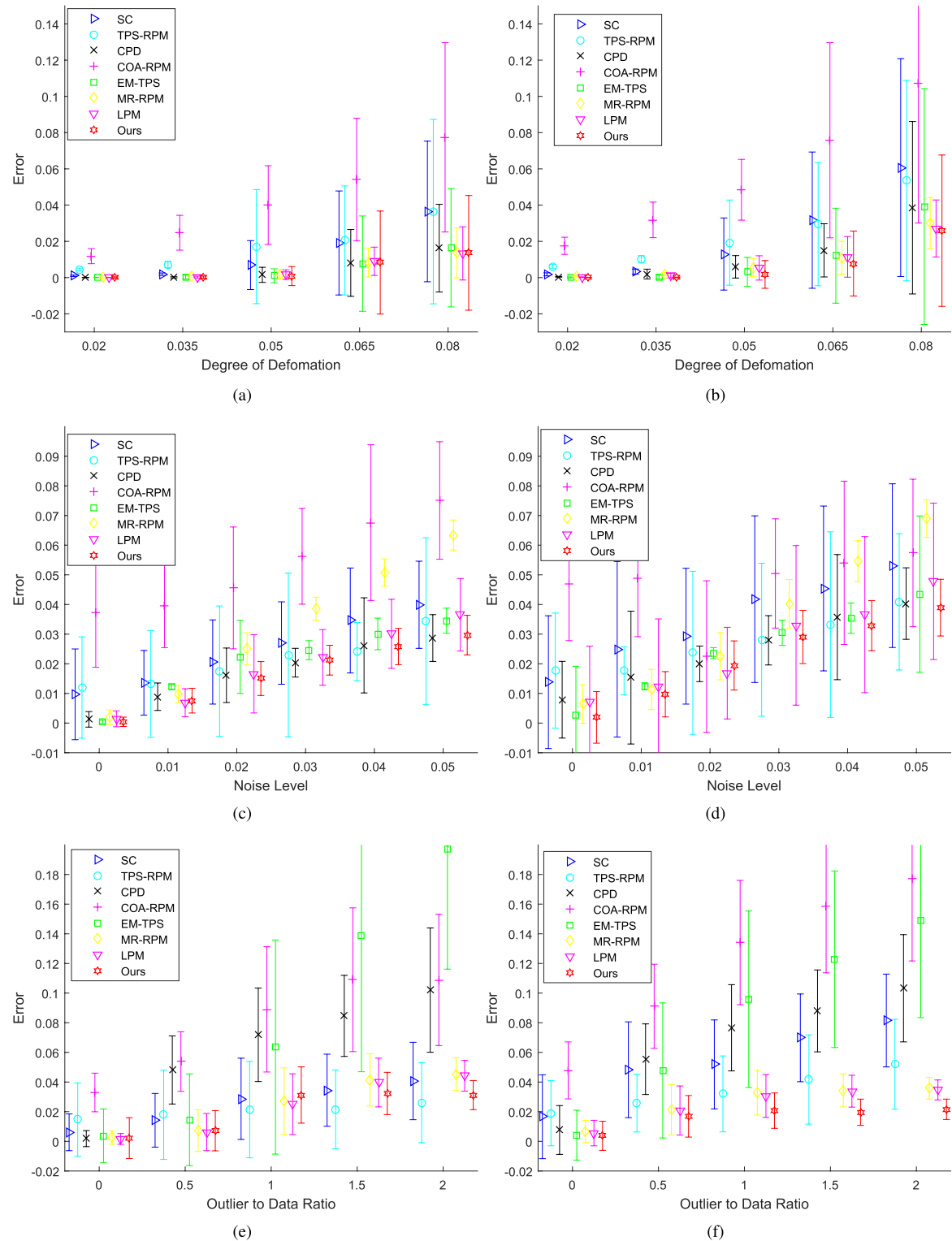


FIGURE 4. Comparison of our method with SC [15], TPS-RPM [5], CPD [16], COA-RPM [34], EM-TPS [12], and MR-RPM [35], [36], and LPM [37] on the fish (left) and Chinese character (right) [5]. The error bars indicate the registration error means and standard deviations over 100 trials.

the registration errors for seven out of the ten sets of data (the fish shapes with deformation, noise, and rotation and the Chinese character shapes with deformation, noise, outliers,

and rotation) and achieves comparable results for the others (the fish shapes with outliers and occlusion and the Chinese character shapes with occlusion). CPD, EM-TPS, MR-RPM,

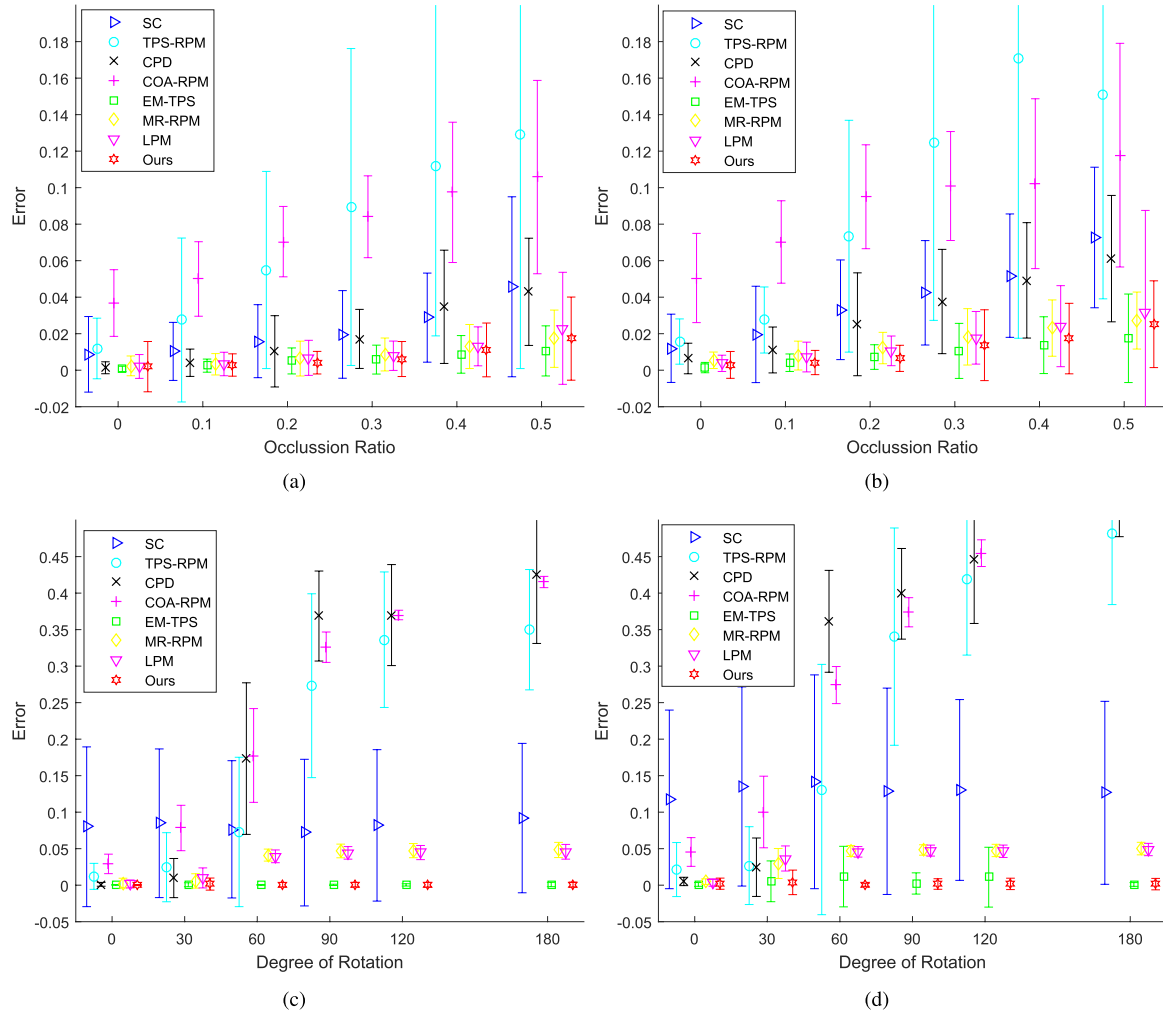


FIGURE 5. Comparison of our method with SC [15], TPS-RPM [5], CPD [16], COA-RPM [34], EM-TPS [12], and MR-RPM [35], [36], and LPM [37] on the fish (left) and Chinese character (right) [33]. The error bars indicate the registration error means and standard deviations over 100 trials.

and LPM achieve low mean of the registration errors for most of the ten sets of data, but EM-TPS achieves the worst registration errors for two sets of data (the fish and Chinese character shapes with outliers), and CPD performs significantly worse than the others for two sets of data (the fish and Chinese character shapes with rotation). SC yields average scores for all the experiments. In many cases, COA-RPM does not perform well.

To determine whether the means of the registration error of all the 100 samples obtained by our method and other methods are statistically significant, the p-values from one-way analysis of variance (ANOVA) statistical test are considered in this paper. Following [38], a significance level of 5% is chosen to compare the p-values to estimate the null hypothesis. If the p-values are $\leq 5\%$, the null hypothesis is rejected. The statistical results between our method versus each registration method are listed in Tables 1 and 2. From Tables 1 and 2, we can see that the population means are not all equal for all cases. Therefore, the null hypotheses can be rejected.

B. EXPERIMENTS WITH MNIST HANDWRITTEN DIGIT DATABASE

In this subsection, we will discuss the evaluation of the performance of the seven point set registration methods (i.e. SC [15], TPS-RPM [5], CPD [16], EM-TPS [12], MR-RPM [35], [36], LPM [37], and our method) on the MNIST handwritten digit database [39] with 10 categories corresponding to the 10 digits (from 0 to 9). Each category includes 1000 images. Each image is 28×28 in size. In the registration test, we use the first sample in each category as the template, and use the rest images as the targets. The ten templates are shown in Fig. 8. In the experiments, the 48 brightest points are sampled from the Canny edges. The correspondence between the template point set and the target point set is established by the registration method. Then, the template shape is warped using the estimated correspondence.

The registration error is quantified as the mean of the Euclidean distance between a point in the target and the corresponding point in the warped template. Table 3 presents

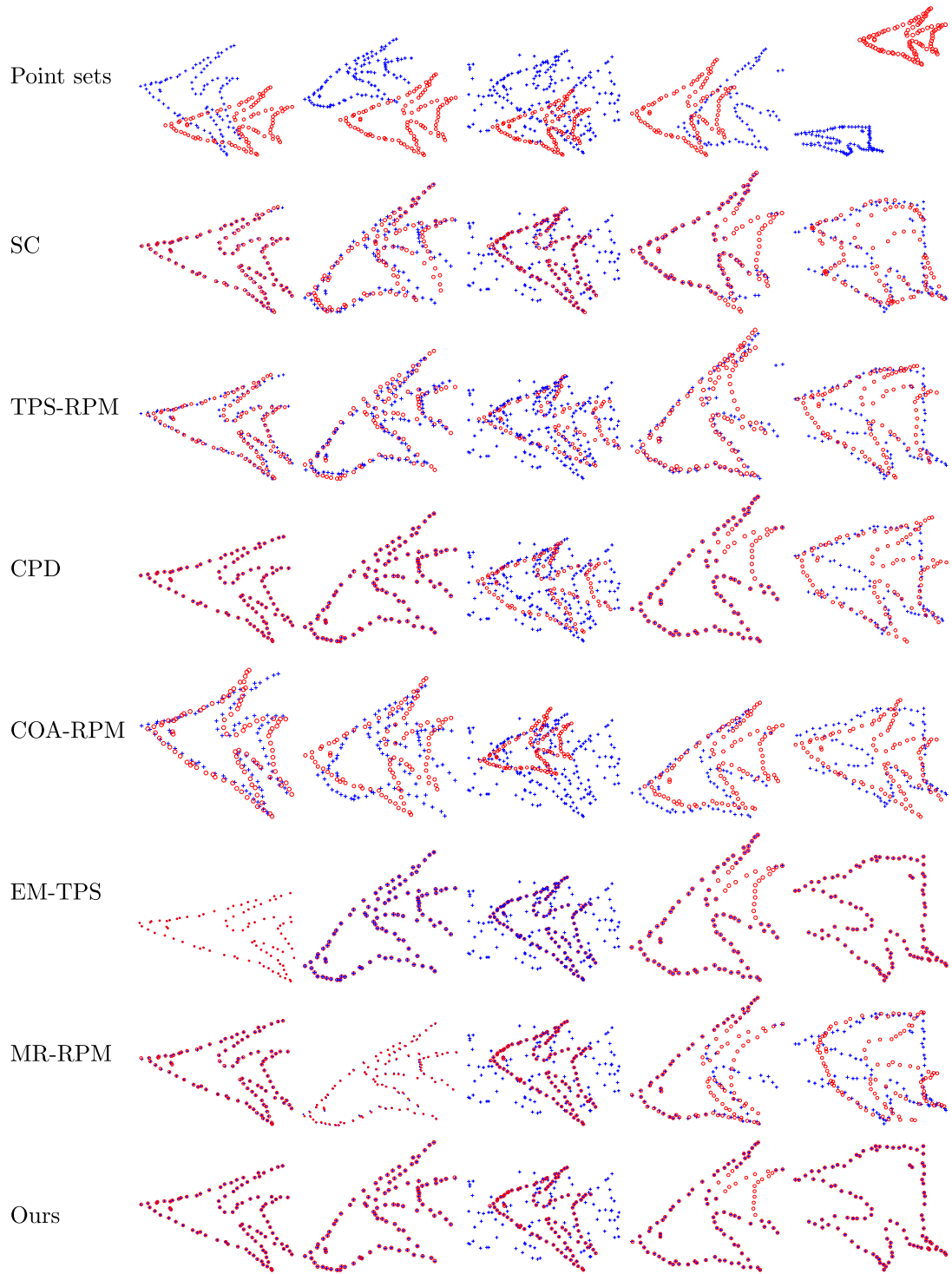


FIGURE 6. Examples of registration results by different methods on the fish shapes (from left to right column) degraded by the deformation, noise, outlier, occlusion, and rotation. Top row: the model (red circles) and target (blue pluses) point sets. From second to bottom row: registration results by SC [15], TPS-RPM [5], CPD [16], COA-RPM [34], EM-TPS [12], MR-RPM [35], [36], LPM [37], and our method, respectively.

the values of the quality of registration error for the seven competing registration methods. From Table 3, we can see that our method shows superiority over the other six competing methods with respect to the performance of the average

registration error. EM-TPS, MR-RPM, and LPM achieve low registration error for the MNIST database. SC and TPS-RPM yield average scores. CPD obtains the worst registration errors in this evaluation.

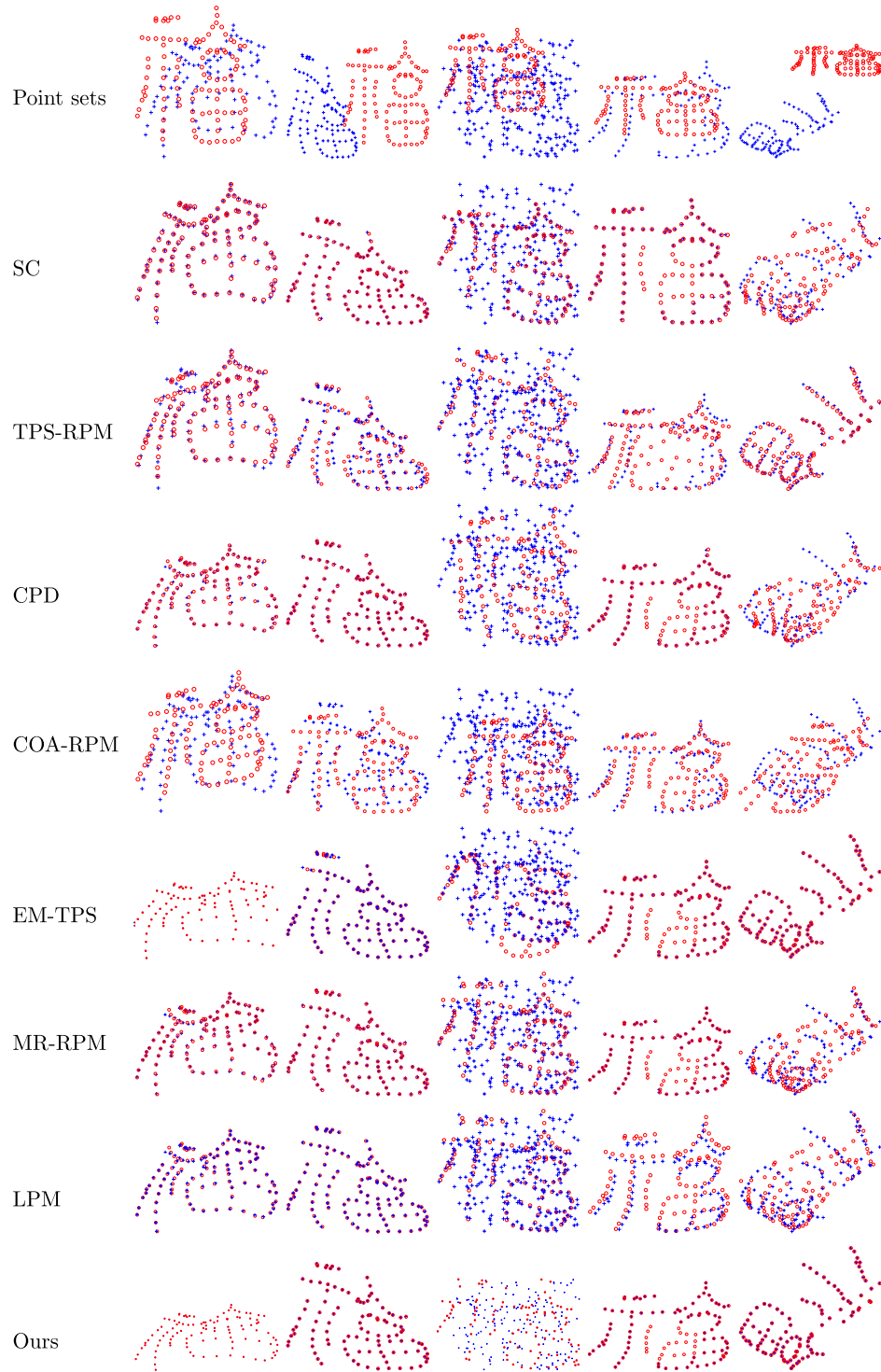


FIGURE 7. Examples of registration results by different methods on the Chinese character shapes (from left to right column) degraded by the deformation, noise, outlier, occlusion, and rotation. Top row: the model (red circles) and target (blue pluses) point sets. From second to bottom row: registration results by SC [15], TPS-RPM [5], CPD [16], COA-RPM [34], EM-TPS [12], MR-RPM [35], [36], LPM [37], and our method, respectively.

C. EXPERIMENTS WITH MPEG-7 SHAPE SILHOUETTE DATABASE

In this subsection, we evaluate the performance of the seven point set registration methods (i.e., SC [15], TPS-RPM [5],

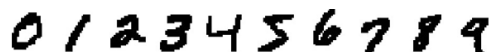
CPD [16], EM-TPS [12], MR-RPM [35], [36], LPM [37], and our method) on the MPEG-7 shape silhouette database [40], particularly the core experiment CE-shape-1 part B, which contains 1400 images from 70 different shapes.

TABLE 1. P-values between our method versus each registration method for the Chinese character shapes.

| Groups | | SC | TPS-RPM | CPD | COA-RPM | EM-TPS | MR-TPS | LPM |
|-------------|-------|--------------|--------------|--------------|--------------|--------------|--------------|--------------|
| Deformation | 0.020 | 0.003 | 0.000 | 0.000 | 0.000 | 0.573 | 0.000 | 0.000 |
| | 0.035 | 0.000 | 0.000 | 0.000 | 0.000 | 0.007 | 0.000 | 0.000 |
| | 0.050 | 0.021 | 0.000 | 0.125 | 0.000 | 0.2033 | 0.00 | 0.000 |
| | 0.065 | 0.095 | 0.103 | 0.5147 | 0.002 | 0.176 | 0.124 | 0.083 |
| | 0.080 | 0.141 | 0.132 | 0.2316 | 0.047 | 0.087 | 0.097 | 0.164 |
| | 0.00 | 0.000 | 0.000 | 0.000 | 0.000 | 0.709 | 0.000 | 0.010 |
| Noise | 0.01 | 0.000 | 0.000 | 0.018 | 0.000 | 0.000 | 0.113 | 0.275 |
| | 0.02 | 0.001 | 0.000 | 0.586 | 0.265 | 0.000 | 0.007 | 0.142 |
| | 0.03 | 0.237 | 0.158 | 0.359 | 0.000 | 0.161 | 0.000 | 0.169 |
| | 0.04 | 0.187 | 0.165 | 0.208 | 0.000 | 0.011 | 0.000 | 0.182 |
| | 0.05 | 0.256 | 0.276 | 0.371 | 0.000 | 0.105 | 0.000 | 0.001 |
| | 0 | 0.031 | 0.011 | 0.042 | 0.000 | 0.823 | 0.019 | 0.161 |
| Outlier | 0.5 | 0.000 | 0.000 | 0.000 | 0.000 | 0.000 | 0.050 | 0.072 |
| | 1 | 0.000 |
| | 1.5 | 0.000 |
| | 2 | 0.000 |
| | 0.00 | 0.000 | 0.000 | 0.002 | 0.000 | 0.064 | 0.004 | 0.319 |
| | 0.1 | 0.000 | 0.000 | 0.000 | 0.000 | 0.901 | 0.000 | 0.005 |
| Occlusion | 0.2 | 0.039 | 0.000 | 0.000 | 0.000 | 0.467 | 0.000 | 0.000 |
| | 0.3 | 0.000 | 0.000 | 0.000 | 0.000 | 0.204 | 0.066 | 0.095 |
| | 0.4 | 0.000 | 0.000 | 0.000 | 0.000 | 0.146 | 0.021 | 0.022 |
| | 0.5 | 0.012 | 0.000 | 0.09 | 0.000 | 0.024 | 0.482 | 0.000 |
| | 0 | 0.003 | 0.000 | 0.000 | 0.000 | 0.212 | 0.001 | 0.0969 |
| | 30 | 0.000 | 0.000 | 0.000 | 0.000 | 0.656 | 0.000 | 0.000 |
| Rotation | 60 | 0.000 | 0.000 | 0.000 | 0.000 | 0.007 | 0.000 | 0.000 |
| | 90 | 0.000 | 0.000 | 0.000 | 0.000 | 0.652 | 0.000 | 0.000 |
| | 120 | 0.000 |
| | 180 | 0.000 | 0.000 | 0.000 | 0.000 | 0.570 | 0.000 | 0.000 |

TABLE 2. P-values between our method versus each registration method for the Fish character shapes.

| Groups | | SC | TPS-RPM | CPD | COA-RPM | EM-TPS | MR-TPS | LPM |
|-------------|-------|--------------|--------------|--------------|--------------|--------------|--------------|--------------|
| Deformation | 0.020 | 0.017 | 0.000 | 0.1517 | 0.000 | 0.019 | 0.020 | 0.150 |
| | 0.035 | 0.000 | 0.000 | 0.017 | 0.000 | 0.556 | 0.000 | 0.427 |
| | 0.050 | 0.061 | 0.087 | 0.307 | 0.000 | 0.820 | 0.0552 | 0.178 |
| | 0.065 | 0.155 | 0.149 | 0.952 | 0.008 | 0.876 | 0.2958 | 0.255 |
| | 0.080 | 0.374 | 0.328 | 0.514 | 0.000 | 0.538 | 0.467 | 0.931 |
| | 0.00 | 0.000 | 0.004 | 0.006 | 0.000 | 0.898 | 0.000 | 0.001 |
| Noise | 0.01 | 0.000 | 0.027 | 0.035 | 0.000 | 0.000 | 0.000 | 0.266 |
| | 0.02 | 0.046 | 0.159 | 0.312 | 0.000 | 0.000 | 0.000 | 0.271 |
| | 0.03 | 0.132 | 0.218 | 0.226 | 0.000 | 0.000 | 0.000 | 0.379 |
| | 0.04 | 0.000 | 0.634 | 0.819 | 0.000 | 0.000 | 0.000 | 0.001 |
| | 0.05 | 0.000 | 0.317 | 0.339 | 0.000 | 0.000 | 0.000 | 0.000 |
| | 0 | 0.571 | 0.379 | 0.829 | 0.000 | 0.509 | 0.842 | 0.693 |
| Outlier | 0.5 | 0.008 | 0.287 | 0.000 | 0.029 | 0.755 | 0.3854 | 0.619 |
| | 1 | 0.000 | 0.047 | 0.000 | 0.000 | 0.1696 | 0.378 | 0.029 |
| | 1.5 | 0.000 | 0.000 | 0.000 | 0.000 | 0.000 | 0.124 | 0.000 |
| | 2 | 0.000 | 0.000 | 0.591 | 0.012 | 0.000 | 0.000 | 0.000 |
| | 0.00 | 0.386 | 0.000 | 0.663 | 0.000 | 0.3672 | 0.772 | 0.949 |
| | 0.1 | 0.257 | 0.000 | 0.203 | 0.000 | 0.6269 | 0.638 | 0.532 |
| Occlusion | 0.2 | 0.005 | 0.000 | 0.002 | 0.000 | 0.049 | 0.581 | 0.021 |
| | 0.3 | 0.000 | 0.000 | 0.000 | 0.000 | 0.801 | 0.059 | 0.152 |
| | 0.4 | 0.000 | 0.000 | 0.000 | 0.000 | 0.175 | 0.327 | 0.281 |
| | 0.5 | 0.000 | 0.000 | 0.000 | 0.000 | 0.012 | 0.985 | 0.000 |
| | 0 | 0.005 | 0.000 | 0.000 | 0.000 | 0.297 | 0.000 | 0.001 |
| | 30 | 0.000 | 0.000 | 0.003 | 0.000 | 0.031 | 0.000 | 0.000 |
| Rotation | 60 | 0.000 | 0.000 | 0.000 | 0.000 | 0.426 | 0.000 | 0.000 |
| | 90 | 0.000 | 0.000 | 0.000 | 0.000 | 0.484 | 0.000 | 0.000 |
| | 120 | 0.000 | 0.000 | 0.000 | 0.000 | 0.714 | 0.000 | 0.000 |
| | 180 | 0.000 | 0.000 | 0.000 | 0.000 | 0.741 | 0.000 | 0.000 |

**FIGURE 8.** The first sample in each category used as template.

Each category has 20 images. The first sample in each category is used as the template, and the rest images are used as the targets for the registration test. Some examples are shown

in Fig. 9. In our evaluation, we first sample 150 brightest points from the silhouette of every shape and run each point matching method to calculate the transformation between two shapes and then use it to warp one of the shapes.

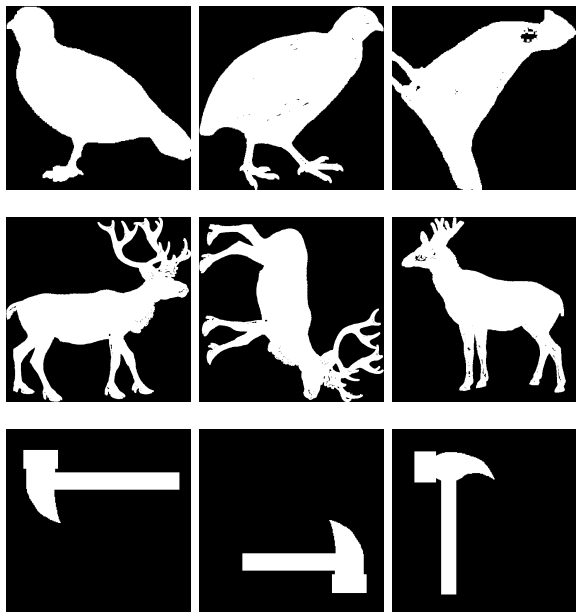
The registration error is quantified as the mean of the Euclidean distance between a point in the target and the corresponding point in the warped template. In some categories,

TABLE 3. Performance comparison on the MNIST database.

| | SC | TPS-RPM | CPD | EM-TPS | MR-TPS | LPM | Ours |
|---------------|--------|---------|--------|--------|--------|--------|---------------|
| Average error | 0.0595 | 0.0511 | 0.0833 | 0.0326 | 0.0275 | 0.0252 | 0.0229 |

TABLE 4. Performance comparison on the MPEG-7 shape silhouette database.

| | SC | TPS-RPM | CPD | EM-TPS | MR-TPS | LPM | Ours |
|---------------|--------|---------|--------|--------|--------|--------|---------------|
| Average error | 0.0448 | 0.0570 | 0.0650 | 0.0845 | 0.0388 | 0.0347 | 0.0316 |

**FIGURE 9.** Examples of shapes in the MPEG-7 database.

the shapes appear to be rotated and flipped. To address this problem, three versions of the template (unchanged, upside-down flipped, and horizontally flipped) are used to match a target, and the smallest error is chosen as the registration error. Table 4 gives the values of the quality of the registration error for the seven competing registration methods. From Table 4, we can see that our method performs the best. The average error of the proposed approach is 0.0316 and is less than that of 0.0448, 0.0570, 0.0650, 0.0845, 0.0388, and 0.0347, respectively, of the SC, TPS-RPM, CPD, EM-TPS, MR-RPM, and LPM methods.

IV. CONCLUSION

In this paper, we propose a novel method for non-rigid registration. The correspondences and the transformation between two point sets are recovered jointly by using the EM algorithm. We have carried out a performance comparison between the proposed approach, SC [15], TPS-RPM [5], CPD [16], COA-RPM [34], EM-TPS [12], MR-RPM [35], [36], LPM [37]. The experimental results on synthetic data as well as real data show that the proposed approach provides slightly better evaluation index values than the state-of-the-art methods. On the basis of the evaluation index value comparison of various registration methods, we can draw a conclusion that the adaptive weighted objective function could effectively recover the underlying transformation.

REFERENCES

- [1] J. Ma, J. Jiang, C. Liu, and Y. Li, "Feature guided Gaussian mixture model with semi-supervised EM and local geometric constraint for retinal image registration," *Inf. Sci.*, vol. 417, pp. 128–142, Nov. 2017.
- [2] Y. Gao, J. Ma, and A. L. Yuille, "Semi-supervised sparse representation based classification for face recognition with insufficient labeled samples," *IEEE Trans. Image Process.*, vol. 26, no. 5, pp. 2545–2560, May 2017.
- [3] L. G. Brown, "A survey of image registration techniques," *ACM Comput. Surv.*, vol. 24, no. 4, pp. 325–376, Dec. 1992.
- [4] P. J. Besl and N. D. McKay, "A method for registration of 3-D shapes," *IEEE Trans. Pattern Anal. Mach. Intell.*, vol. 14, no. 2, pp. 239–256, Feb. 1992.
- [5] H. Chui and A. Rangarajan, "A new point matching algorithm for non-rigid registration," *Comput. Vis. Image Understand.*, vol. 89, nos. 2–3, pp. 114–141, Feb./Mar. 2003.
- [6] J. Ma, J. Zhao, and A. L. Yuille, "Non-rigid point set registration by preserving global and local structures," *IEEE Trans. Image Process.*, vol. 25, no. 1, pp. 53–64, Jan. 2016.
- [7] J. Ma, J. Jiang, H. Zhou, J. Zhao, and X. Guo, "Guided locality preserving feature matching for remote sensing image registration," *IEEE Trans. Geosci. Remote Sens.*, vol. 56, no. 8, pp. 4435–4447, Aug. 2018.
- [8] J. Ma, C. Chen, C. Li, and J. Huang, "Infrared and visible image fusion via gradient transfer and total variation minimization," *Inf. Fusion*, vol. 31, pp. 100–109, Sep. 2016.
- [9] R. Hartley and A. Zisserman, *Multiple View Geometry in Computer Vision*, 2nd ed. Cambridge, U.K.: Cambridge Univ. Press, 2003.
- [10] Z. Chen, X. Sun, L. Wang, Y. Yu, and C. Huang, "A deep visual correspondence embedding model for stereo matching costs," in *Proc. IEEE Int. Conf. Comput. Vis. (ICCV)*, Dec. 2015, pp. 972–980.
- [11] A. W. Fitzgibbon, "Robust registration of 2D and 3D point sets," *Image Vis. Comput.*, vol. 21, nos. 13–14, pp. 1145–1153, Dec. 2003.
- [12] J. Chen, J. Ma, C. Yang, L. Ma, and S. Zheng, "Non-rigid point set registration via coherent spatial mapping," *Signal Process.*, vol. 106, pp. 62–72, Jan. 2015.
- [13] C. Yang, M. Zhang, Z. Zhang, L. Wei, R. Chen, and H. Zhou, "Non-rigid point set registration via global and local constraints," *Multimedia Tools Appl.*, vol. 77, no. 24, pp. 31607–31625, 2018.
- [14] J. Ma and J. Zhao, "Robust topological navigation via convolutional neural network feature and sharpness measure," *IEEE Access*, vol. 5, pp. 20707–20715, 2017.
- [15] S. Belongie, J. Malik, and J. Puzicha, "Shape matching and object recognition using shape contexts," *IEEE Trans. Pattern Anal. Mach. Intell.*, vol. 24, no. 4, pp. 509–522, Apr. 2002.
- [16] A. Myronenko and X. Song, "Point set registration: Coherent point drift," *IEEE Trans. Pattern Anal. Mach. Intell.*, vol. 32, no. 12, pp. 2262–2275, Dec. 2010.
- [17] J. Dou, D. Niu, Z. Feng, and X. Zhao, "Robust non-rigid point set registration method based on asymmetric Gaussian and structural feature," *IET Comput. Vis.*, vol. 12, no. 6, pp. 806–816, 2018.
- [18] Z. Zhou et al., "Accurate and robust non-rigid point set registration using student's-t mixture model with prior probability modeling," *Sci. Rep.*, vol. 8, no. 1, p. 8742, 2018.
- [19] J. Ma, J. Zhao, J. Tian, A. L. Yuille, and Z. Tu, "Robust point matching via vector field consensus," *IEEE Trans. Image Process.*, vol. 23, no. 4, pp. 1706–1721, Apr. 2014.
- [20] J. Ma, J. Zhao, J. Tian, X. Bai, and Z. Tu, "Regularized vector field learning with sparse approximation for mismatch removal," *Pattern Recognit.*, vol. 46, no. 12, pp. 3519–3532, 2013.
- [21] H. Zhou, J. Ma, C. Yang, S. Sun, R. Liu, and J. Zhao, "Nonrigid feature matching for remote sensing images via probabilistic inference with global and local regularizations," *IEEE Geosci. Remote Sens. Lett.*, vol. 13, no. 3, pp. 374–378, Mar. 2016.

- [22] J. Yan, M. Cho, H. Zha, X. Yang, and S. M. Chu, "Multi-graph matching via affinity optimization with graduated consistency regularization," *IEEE Trans. Pattern Anal. Mach. Intell.*, vol. 38, no. 6, pp. 1228–1242, Jun. 2016.
- [23] W. Lian, L. Zhang, and M.-H. Yang, "An efficient globally optimal algorithm for asymmetric point matching," *IEEE Trans. Pattern Anal. Mach. Intell.*, vol. 39, no. 7, pp. 1281–1293, Jul. 2017.
- [24] J. Yan, C. Li, Y. Li, and G. Cao, "Adaptive discrete hypergraph matching," *IEEE Trans. Cybern.*, vol. 48, no. 2, pp. 765–779, Feb. 2018.
- [25] L. Bai, X. Yang, and H. Gao, "Nonrigid point set registration by preserving local connectivity," *IEEE Trans. Cybern.*, vol. 48, no. 3, pp. 826–835, Mar. 2018.
- [26] B. Jian and B. C. Vemuri, "Robust point set registration using Gaussian mixture models," *IEEE Trans. Pattern Anal. Mach. Intell.*, vol. 33, no. 8, pp. 1633–1645, Aug. 2011.
- [27] J. Ma, H. Zhou, J. Zhao, Y. Gao, J. Jiang, and J. Tian, "Robust feature matching for remote sensing image registration via locally linear transforming," *IEEE Trans. Geosci. Remote Sens.*, vol. 53, no. 12, pp. 6469–6481, Dec. 2015.
- [28] J. Ma, W. Qiu, J. Zhao, Y. Ma, A. L. Yuille, and Z. Tu, "Robust L_2E estimation of transformation for non-rigid registration," *IEEE Trans. Signal Process.*, vol. 63, no. 5, pp. 1115–1129, Mar. 2015.
- [29] G. Wahba, *Spline Models for Observational Data*. Philadelphia, PA, USA: SIAM, 1990.
- [30] C. M. Bishop, *Pattern Recognition and Machine Learning*. New York, NY, USA: Springer-Verlag, 2006.
- [31] A. P. Dempster, N. M. Laird, and D. B. Rubin, "Maximum likelihood from incomplete data via the EM algorithm," *J. Roy. Statist. Soc. B, Methodol.*, vol. 39, no. 1, pp. 1–38, 1977.
- [32] H. Zhou et al., "Image deformation with vector-field interpolation based on MRLS-TPS," *IEEE Access*, to be published, doi: [10.1109/ACCESS.2018.2876884](https://doi.org/10.1109/ACCESS.2018.2876884).
- [33] Y. Zheng and D. Doermann, "Robust point matching for nonrigid shapes by preserving local neighborhood structures," *IEEE Trans. Pattern Anal. Mach. Intell.*, vol. 28, no. 4, pp. 643–649, Apr. 2006.
- [34] W. Lian and L. Zhang, "Robust point matching revisited: A concave optimization approach," in *Proc. Eur. Conf. Comput. Vis.*, 2012, pp. 259–272.
- [35] J. Ma, J. Zhao, J. Jiang, and H. Zhou, "Non-rigid point set registration with robust transformation estimation under manifold regularization," in *Proc. 34th AAAI Conf. Artif. Intell.* Menlo Park, CA, USA: AAAI, 2017, pp. 4218–4224.
- [36] J. Ma, J. Wu, J. Zhao, J. Jiang, H. Zhou, and Q. Z. Sheng, "Nonrigid point set registration with robust transformation learning under manifold regularization," *IEEE Trans. Neural Netw. Learn. Syst.*, to be published, doi: [10.1109/TNNLS.2018.2872528](https://doi.org/10.1109/TNNLS.2018.2872528).
- [37] J. Ma, J. Zhao, J. Jiang, H. Zhou, and X. Guo, "Locality preserving matching," *Int. J. Comput. Vis.*, to be published, doi: [10.1007/s11263-018-1117-z](https://doi.org/10.1007/s11263-018-1117-z).
- [38] B. M. Mahmood, A. R. B. Ramli, S. H. Abdulhussain, S. A. R. Al-Haddad, and W. A. Jassim, "Signal compression and enhancement using a new orthogonal-polynomial-based discrete transform," *IET Signal Process.*, vol. 12, no. 1, pp. 129–142, 2018.
- [39] Y. LeCun, L. Bottou, Y. Bengio, and P. Haffner, "Gradient-based learning applied to document recognition," *Proc. IEEE*, vol. 86, no. 11, pp. 2278–2324, Nov. 1998.
- [40] S. Jeannin and M. Bober, *Description of Core Experiments for MPEG-7 Motion/Shape*, document ISO/IEC JTC 1/SC 29/WG 11 MPEG99/N2690, MPEG-7, Seoul, South Korea, Mar. 1999.



YIZHANG LIU received the B.S. degree in electronic information engineering from Fujian Agriculture and Forestry University, Fuzhou, China, in 2017, where he is currently pursuing the master's degree in computer science. His current research interests include computer vision and image matching.



XINGYU JIANG received the B.E. degree from the Department of Mechanical and Electronic Engineering, Huazhong Agricultural University, Wuhan, China, in 2017. He is currently pursuing the master's degree with the Electronic Information School, Wuhan University, Wuhan. His current research interests include computer vision, machine learning, and pattern recognition.



ZEJUN ZHANG received the B.S. and M.S. degrees in computer science from GuiZhou University, GuiYang, China, in 2007 and 2010, respectively, and the Ph.D. degree in electronic engineering from Xidian University, Xi'an, China, in 2014. He is currently a Lecturer with the College of Computer and Information Sciences, Fujian Agriculture and Forestry University, Fuzhou, China. His current research interests include pattern recognition and synthetic aperture radar image processing.



LIFANG WEI received the bachelor's degree in electronic communication engineering from Xi'an Shiyou University, Xi'an, China, in 2005, the master's degree in biomedical engineering from Northwestern Polytechnical University, Xi'an, in 2008, and the Ph.D. degree in communication and information system from Fuzhou University, Fuzhou, China, in 2013. She is currently an Associate Professor with the College of Computer and Information, Fujian Agriculture and Forestry University, Fuzhou. Her research interests include computer vision and image processing.



CHANGCAI YANG received the M.S. degree in control theory and control engineering from China Three Gorges University, China, in 2008, and the Ph.D. degree in pattern recognition and intelligent systems from the Huazhong University of Science and Technology (HUST), China, in 2012. From 2012 to 2014, he held a post-doctoral position at HUST. Since 2016, he has been an Associate Professor and the M.S. Supervisor with the College of Computer and Information Science, Fujian Agriculture and Forestry University, Fuzhou, China. He has published more than 30 papers. His research interests include computer vision, image processing, and point set registration.



TAOTAO LAI received the Ph.D. degree in computer science and technology from Xiamen University, Xiamen, China, in 2016. Since 2017, he has been a Post-Doctoral Fellow with Fujian Agriculture and Forestry University. He has published several papers in international journals, including the *IEEE TRANSACTIONS ON INTELLIGENT TRANSPORTATION SYSTEMS*, *Pattern Recognition*, and *Computer Vision and Image Understanding*. His research interests include structure from motion and robust model fitting.



RIQING CHEN received the B.Eng. degree in communication engineering from Tongji University, China, in 2001, the M.Sc. degree in communications and signal processing from Imperial College London, U.K., in 2004, and the Ph.D. degree in engineering science from the University of Oxford, U.K., in 2010. Since 2014, he has been a Professor and the M.S. Supervisor with the College of Computer and Information Science, Fujian Agriculture and Forestry University, Fuzhou, China. His current research interests include big data and visualization, cloud computing, consumer electronics, flash memory, wireless sensor networking, and image processing.

• • •